Development of a new method for Pb isotopic analysis of archaeological artefacts using single-collector ICP-dynamic reaction cell-MS

David De Muynck,* Christophe Cloquet and Frank Vanhaecke

Received 21st June 2007, Accepted 14th August 2007
First published as an Advance Article on the web 29th August 2007
DOI: 10.1039/b709461b

A new methodology has been developed for Pb isotopic analysis of different kinds of archaeological artefacts. The method has been optimized for bone tissue, soil, amphorae and lead objects dating from the Roman Era, and consists of 3 key steps: (i) sample digestion with quantitative Pb recovery, optimized using the certified reference materials NIST SRM 1400 Bone Ash, BCR CRM 141 Calcareous Loam Soil and BCR CRM 142 Light Sandy Soil, (ii) quantitative isolation of the pure Pb fraction and (iii) isotope ratio measurement with a quadrupole-based ICP-mass spectrometer, equipped with a dynamic reaction cell (DRC). For Pb isolation, an extraction chromatographic column, containing a resin with a Pb-selective crown ether (4,4′(5′)-di-*tert*-butylcyclohexane-18-crown-6) purchased from Eichrom Technologies, was used. The Pb fraction can be obtained in a pure form and in a quantitative way after a relatively fast process, the columns can be reused and no Pb isotopic fractionation occurs on the column. The isolation process has been validated using NIST SRM 981 Common Lead, and by application to samples with a known isotopic composition. For isotope ratio measurements, the use of Ne as a collision gas in the DRC allowed an external precision below 0.17% RSD for the $^{X}Pb/^{204}Pb$ ratios (where $X = 206, 207, 208$) and below 0.09% RSD for the $^{207}Pb/^{206}Pb$, $^{208}Pb/^{206}Pb$ and $^{208}Pb/^{207}Pb$ ratios to be obtained. The accuracy of the measurement protocol was validated by comparing the results thus obtained with the corresponding MC-ICP-MS and TI-MS values. Pb isotope ratios for the certified reference materials used are given. The method was also demonstrated to work for a totally different kind of (complex) sample (lichen), and thus it is expected that the method can be used for Pb isotope ratio analysis of a wide variety of materials.

1. Introduction

Among the mass spectrometric techniques developed in the 20th century, thermal ionisation-mass spectrometry (TI-MS) has been established as the reference technique for high-precision isotope ratio determinations of the heavier elements.[1] Since its commercial introduction in 1983, inductively coupled plasma-mass spectrometry (ICP-MS) has gained more and more importance as a technique for trace analysis and isotope ratio determination. For isotope ratio applications where an extremely good precision is not necessary, single-collector ICP-MS (SC-ICP-MS) offers important benefits over TI-MS, *e.g.*, the continuous nebulisation of sample solution (at the cost of a larger sample consumption) in an ion source at atmospheric pressure, the higher sample throughput and the high ionisation efficiency of the ICP. However, in traditional quadrupole-based ICP-MS, the isotope ratio precision is limited to 0.1–0.5% RSD.[2] The occurrence of spectral interferences is another drawback, further limiting the application field of quadrupole-based ICP-MS for isotopic studies. Double focusing sector field ICP-MS can be operated at an increased mass resolution, permitting the analyte signals to be resolved from those of isobaric molecular ions[3] and provides an isotope ratio precision of 0.05–0.2% RSD.[2] In quadrupole-based ICP-MS, considerable progress has been made in terms of both precision and the battle against interferences by the introduction of the dynamic reaction cell (DRC) and other types of collision/reaction cells,[4–7] resulting in a better isotope ratio precision (~0.05% RSD).[8] Unfortunately, the use of a reaction- or collision gas in the cell has a significant influence on the mass discrimination.[9] In order to obtain accurate results, an adequate mass discrimination correction is necessary, and thus it was stated that the isolation of the target element prior to isotope ratio analysis is highly recommended. Furthermore, in case of low analyte concentrations—even when the DRC is used under vented conditions (no gas in the cell)—a preliminary target element isolation, and thus preconcentration, can improve the isotope ratio precision obtained. Following Poisson counting statistics, theoretically a higher precision is attainable at higher analyte concentrations (count rates).

Isolation methods preceding an isotopic analysis can introduce isotopic fractionation, as observed for elements like Fe,[10] Cu and Zn[11] and Cd.[12] Isotopic fractionation of Pb has not been observed yet, mainly due to its high mass. In any way, a quantitative target element recovery for the isolation process is

Ghent University, Department of Analytical Chemistry, Krijgslaan 281-S12, B-9000 Ghent, Belgium. E-mail: David.DeMuynck@UGent.be

a guarantee to prevent isotopic fractionation during the sample pre-treatment from occurring.

The methodology described later on has been developed for a multidisciplinary research project concerning the investigation of possible lead poisoning in the population of a Roman settlement. The samples subject to investigation are infant bone tissue and surrounding soil samples, along with possible sources of bone lead, such as amphorae and lead objects dating from the Roman Era. Due to the radioactive decay of the naturally occurring and long-lived radionuclides ^{232}Th, ^{235}U and ^{238}U into ^{208}Pb, ^{207}Pb and ^{206}Pb, respectively, lead shows quite a large variation in isotopic composition.[13] This makes Pb isotopic analysis a powerful tool to conduct the studies described above. Pb isotopic analysis of bone and similar tissues, *e.g.*, teeth, and surrounding soils, has already been used for conducting archaeological studies.[14–17]

2. Experimental

2.1 Reagents and materials

Pro analysi nitric acid (14 M) and hydrochloric acid (12 M) (Panreac, Spain) were further purified by subboiling distillation in quartz equipment. Hydrofluoric acid (22 M, instra-analyzed) and perchloric acid (10 M, instra-analyzed) were bought from J.T. Baker Chemicals N.V., The Netherlands. Ultrapure water with a resistivity >18 MΩ cm was obtained from a Milli-Q system (Millipore, USA) and used throughout this work for preparing dilutions. *Pro analysi* ammonium-oxalate—$(NH_4)_2C_2O_4 \cdot 2H_2O$—was purchased from UCB, Belgium. Standard solutions for elemental assay were prepared by diluting commercially available single element 1 g L^{-1} stock solutions (Alfa Johnson-Matthey, Germany). NIST SRM 981 Common Lead (National Institute for Standards and Technology, USA) was used as an isotopic standard. Lead extraction chromatographic columns (Pb spec™) were purchased from Eichrom Environment, France. Argon for ICP-MS measurements had a purity $>99.999\%$ and was supplied by Air Liquide, Belgium. Neon with a purity $>99.997\%$ was supplied by Air Products, Belgium.

For sample digestions, a Milestone microwave labstation MLS-1200 mega equipped with MDR™ technology (microwave destruction rotor) was used. The microwave vessels made from tetrafluoromethaxil (TFM) were cleaned after every use by filling them with the same combination of acids as used for sample digestion and submitting them to the digestion programme, followed by rinsing with Milli-Q water and drying in an oven at 105 °C. Beakers used for digestion on a hotplate were manufactured from teflon and were cleaned after every use by boiling in aqua regia for 6 h, subsequent boiling in Milli-Q water for another 6 h, and were finally dried in an oven at 105 °C.

2.2 Instrumentation

Elemental assays and semi-quantitative analyses were carried out using a quadrupole-based Perkin–Elmer SCIEX Elan 5000 ICP-MS. The instrumental settings and data acquisition parameters for this instrument are summarized in Table 1. The sample introduction system consisted of a multi-channel peristaltic pump (Minipuls-3), a GemTip cross-flow nebulizer, a Perkin–Elmer Type II spray chamber made of Ryton, and a Perkin–Elmer corrosion-resistant torch with alumina injector.

Table 1 Instrumental settings and data acquisition parameters for the ICP-mass spectrometers used

	Elan 5000	Elan DRC*plus*
Instrumental settings		
RF power/W	1000	1200
Plasma gas flow rate/L min^{-1}	15	17
Auxiliary gas flow rate/L min^{-1}	0.8	1.2
Nebulizer gas flow rate/L min^{-1}	0.80–0.85[a]	0.95–1.00[a]
Sampling cone	Ni, aperture diameter 1.0 mm	Ni, aperture diameter 1.1 mm
Skimmer	Ni, aperture diameter 1.0 mm	Ni, aperture diameter 0.9 mm
Sample uptake rate/mL min^{-1}	1	1
Extraction lens voltage/V	N/A	10–12[a]
Data acquisition parameters		
Scanning mode	Peak hopping	Peak hopping
Dwell time/ms	50	2
Settling time/ms	5	0.2
Sweeps	20	500
Readings	3	10
Replicates	3	15, 6 to 15 taken into account
Replicate time/s	10/isotope	46
Detector dead time/ns	69	61
DRC parameters		
Collision gas flow rate/mL min^{-1}	—	0.1[b]
RPa	—	0
RPq	—	0.45

[a] Daily optimized for maximum $^{208}Pb^+$ signal intensity. [b] Actual gas flow rate, conversion factor for the flow rate in Elan units as given by the software equals 1 for noble gases.

Single-collector ICP-MS isotope ratio determinations were carried out using a Perkin–Elmer SCIEX Elan DRC*plus*, equipped with a dynamic reaction cell (DRC). This DRC is located in-between the interface and the mass analyzer and consists of a quadrupole set-up in a closed cell that can be pressurized with either a non-reactive collision gas, or a well-selected reaction gas. When a non-reactive collision gas (*e.g.*, Ne, Ar) is used, ions extracted from the ICP on slightly different moments are mixed in the cell, thereby mitigating the effect of short-term fluctuations on the measured isotope ratio and resulting in a better isotope ratio precision.[8,18] When the DRC is pressurized with a reaction gas (*e.g.*, NH_3, CO), the occurrence of spectral interferences is avoided by selective ion–molecule reactions, in which interfering ions can be converted to non-interfering ions or neutral species.[19] Another possibility is the conversion of the analyte ions into molecular ions with a higher mass-to-charge ratio, followed by interference-free isotope ratio determination at those higher mass-to-charge ratios.[20] Furthermore, the quadrupole-assembly in the DRC allows efficient elimination of newly formed ions in the cell by dynamic bandpass tuning (DBT).[21] For the isotope ratio determinations reported on in this work, the DRC was

pressurized with Ne. The Ne serves as a collision gas, aiming at an improved Pb isotope ratio precision compared to that attainable with standard quadrupole-based ICP-MS. No spectral interferences (*e.g.*, Hg) occurred on the Pb signals obtained for the samples under investigation. The instrumental settings and data acquisition parameters for the Perkin–Elmer SCIEX Elan DRC*plus* are summarized in Table 1. The sample introduction system consisted of a multi-channel peristaltic pump, a Meinhard concentric nebulizer mounted onto a cyclonic spray chamber, and a Perkin–Elmer quartz torch with a quartz injector.

2.3 Development and validation of digestion procedures

The lead objects were partially cut into curls, rinsed with diluted HNO_3, to remove eventual contamination present due to the cutting process, dried in an oven at 105 °C and dissolved using 20 mL of 1.4 M HNO_3 in a beaker on a hotplate. The digestion procedure developed for bone tissue is a modification of the one given by Hinners *et al.*[22] Several soil digestion procedures based on HF and described in literature[23–25] were tested, but unfortunately, none of these resulted in a complete sample digestion. Finally, a digestion procedure described by Riondato *et al.*,[26] wherein a combination of HF and $HClO_4$ is used, was successful. Prior to digestion, the bone, soil and amphora samples were ground to a homogeneous fine powder using a microdismembrator (Mikro-Dismembrator II, Braun, Germany). Approximately 0.2 g was weighed and digested in a three-step procedure (Table 2). The first step in the digestion procedure consisted of a microwave-assisted acid digestion. Since the dissolution was not complete after this microwave step, the digest was transferred to a beaker, and further digested and evaporated to dryness on a hotplate. For the soil samples, additional acid was added to the digest in the beaker. After this second step, complete dissolution of the sample was obtained, and furthermore, corrosive acids such as HF were removed from the sample. In the third step, the remaining gel was taken up in 14 M HNO_3 under ultrasonic agitation, followed by dilution with Milli-Q water to a HNO_3 concentration of 1 M, which is necessary for the subsequent isolation of lead.

The sample digestion procedures were validated using certified reference materials (Table 3). Pb concentrations were determined after sample digestion, and the Pb recovery was calculated. The experimental Pb concentrations and Pb recoveries reported (Table 3) are the mean values for 7 separate digestions, and the uncertainties are expressed as 95% confidence intervals calculated from the 7 replicates. For bone tissue, NIST SRM 1400 Bone Ash and NIST SRM 1486 Bone Meal were used. The experimental Pb recovery equals 98.4 ± 3.6% for NIST SRM 1400 Bone Ash and 99.7 ± 7.2% for NIST SRM 1486 Bone Meal. For soil, BCR CRM 141 Calcareous Loam Soil and BCR CRM 142 Light Sandy Soil were used. The experimental Pb recoveries were 94.9 ± 5.5% for BCR CRM 141 Calcareous Loam Soil and 98.9 ± 6.3% for BCR CRM 142 Light Sandy Soil. The digestion procedure for amphorae was not optimized using a certified reference material because (i) in NIST SRM 679 Brick Clay—presumably the best suited reference material—the lead content is not certified. To the best of the author's knowledge, there is no similar reference material with a certified lead content, and (ii) the elemental composition of these materials is not only very complex, but also shows substantial differences from one material to the other, as shown in several previous studies.[27–30] A quantitative Pb recovery was assumed, based on the visual observation that no more particles were observed in the solution after the entire digestion procedure.

Table 2 Digestion procedures for the artefacts investigated

	Acids (ratio)	Microwave digestion programme
Step 1: microwave-assisted acid digestion		
Amphorae	HNO_3: HCl : HF (3 : 1 : 5)	10 min 250 W, 10 min 600 W, 10 min 250 W
Bone tissue	HNO_3 : HCl (4 : 1)	5 min 250 W, 5 min 400 W, 5 min 250 W
Soil	HNO_3 : HCl : HF (5 : 2 : 2), cool down + $HClO_4$ (1)	20 min 250 W, 8 min 600 W, 15 min 250 W 20 min 250 W, 8 min 400 W, 15 min 250 W
Step 2: further digestion and evaporation on hotplate		
Amphorae & bone tissue	No additional acid	
Soil	Digest + HNO_3 : HF : $HClO_4$ (1 : 1 : 1)	
Step 3: redissolution of the residue		
Amphorae, bone tissue & soil	Take up in concentrated HNO_3 under ultrasonic agitation and dilution to 1 M HNO_3	
Lead objects	Dissolution in 1.4 M HNO_3 on hotplate	

2.4 Development of a Pb isolation procedure

For geological Pb isotope ratio applications, the isolation method described by Manhès *et al.*[31] is considered as the standard method. In this work however, the performance of an extraction chromatographic column, containing a crown ether-based resin, was evaluated. These columns allow the loading of a large amount of samples with a complex matrix

Table 3 Experimental Pb concentration and Pb recovery for 4 certified reference materials, processed according to the digestion procedures developed. The experimental result represents the mean value obtained from 7 separate digestions of each reference material. The experimental uncertainty represents a 95% confidence interval

	$[Pb]_{certified}$/μg g^{-1}	$[Pb]_{experimental}$/μg g^{-1}	Pb recovery (%)
Bone tissue			
NIST SRM 1400 Bone Ash	9.07 ± 0.12	8.92 ± 0.33	98.4 ± 3.6
NIST SRM 1486 Bone Meal	1.335 ± 0.014	1.330 ± 0.097	99.7 ± 7.2
Soil			
BCR CRM 141 Calcareous Loam Soil	29.4 ± 2.6	27.91 ± 1.61	94.9 ± 5.5
BCR CRM 142 Light Sandy Soil	37.8 ± 1.9	37.39 ± 2.40	98.9 ± 6.3

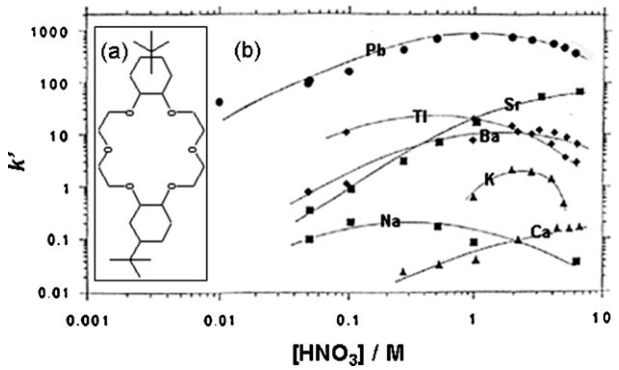

Fig. 1 (a) Pb selective crown ether, 4,4′(5′)-di-*tert*-butylcyclohexane-18-crown-6; (b) Binding properties of Pb and matrix elements on Pb spec™ (modified from Horwitz *et al.*,[32] reprinted with permission).

composition, such as bone tissue. An advantage is the use of less harmful chemicals for column rinsing and elution.

Description of the resin. The Pb spec™ resin used is available in pre-packed 2 mL columns, packed with an inert polymeric carrier with a particle size of 100–150 μm. The crown ether, 4,4′(5′)-di-*tert*-butylcyclohexane-18-crown-6 (Fig. 1a), is present in a 0.75 M concentration in isodecanol, and the inert chromatographic support is loaded with 40% (w/w) of this organic solution. The specific combination of crown ether concentration and alcohol constitutes the resin's selectivity for lead. Pb spec™ columns are derived from a Sr-selective resin (Sr spec™), containing the same crown ether in a 1.0 M concentration and dissolved in 1-octanol. Hence, lead also binds onto Sr spec™ (and *vice versa*), although Sr spec™ displays a lower lead affinity than Pb spec™. Additional information on Eichrom Pb and Sr resins can be found in Horwitz *et al.*[32] and Pin and Bassin,[33] respectively.

Optimization of the use of Pb spec™. The binding properties of Pb and various other elements on Pb spec™ are shown in Fig. 1b. Considering the major elemental composition of the samples studied, especially the data for Na, K, Ca, Sr and Ba are useful. Since Tl is often used for internal mass discrimination correction in the case of Pb isotopic analysis,[34–36] its absence after the Pb isolation procedure has to be guaranteed. Although Tl levels in bone and soil are (very) low, the efficiency of Tl removal has been experimentally evaluated. The capacity factor (k') for Tl remains constant in the range of 0.1 to 1.0 M HNO_3. Na, K and especially Ca are major constituents of bone tissue, Sr is present in trace element range (although at a higher level than Pb) and Ba is present as a trace element in soils. The column shows affinity for Sr and Ba. No data are available for, *e.g.*, Fe and Zn (soil) and Mg (bone). The capacity factor k' is below 1 for K and below 0.1 for Na and Ca in the given HNO_3 concentration range. At 1.0 M HNO_3, k'_{Pb} reaches its maximum value ($\sim 10^3$), so this is the optimum HNO_3 concentration for sample loading onto the column. Sr and Ba are slightly retained under these conditions ($k'_{Sr} \sim 20$ and $k'_{Ba} \sim 10$), but they are removed by rinsing the column with 0.1 M HNO_3 ($k'_{Sr} \sim 1$ and $k'_{Ba} \sim 2$), while k'_{Pb} remains high, $\sim 3 \times 10^2$. As a consequence, the following strategy was suggested: (i) loading the sample in 1.0 M HNO_3 onto the column, (ii) rinsing the column with 20 mL (arbitrary volume, optimized later on) 0.1 M HNO_3 to remove unbound and slightly retained matrix elements (= matrix removal) and (iii) elution of the pure Pb fraction with 20 mL (arbitrary volume, optimized later on) of a suited eluent.

The following experiment was set up: 10 μg Pb from a Pb standard solution in 1.0 M HNO_3 was loaded onto a column, followed by column rinsing with 20 mL 0.1 M HNO_3. The performance in terms of recovery for several eluent candidates given by Horwitz *et al.*[32] was evaluated. With 20 mL Milli-Q water, only 0.38% of the Pb amount was recovered. Next, 20 mL 0.1 M Na_4EDTA solution at pH 7.5 was tested. A major drawback for this application is the strong complexing property of EDTA, resulting in many impurities present in the solution, and Pb blank values of $\sim$100 ng Pb. Furthermore, due to its organic character, it causes strong matrix effects—more specifically, signal suppression—in ICP-MS measurements of up to 35% for Pb. The next candidate was a 0.05 M $(NH_4)_2C_2O_4$ solution. A Pb blank value of 5 ng was found, while other impurities were only present at negligible levels. The signal suppression on the Pb signal due to ammoniumoxalate equals 0–0.5% for 0.05 M $(NH_4)_2C_2O_4$ (the highest concentration used for Pb isotope ratio measurements). The first experiment with a 0.05 M $(NH_4)_2C_2O_4$ solution as eluent resulted in a quantitative Pb recovery. As a consequence, this solution was selected as the best suited eluent for further use.

The next step in the optimization was the determination of the volumes of 0.1 M HNO_3 and 0.05 M $(NH_4)_2C_2O_4$ solution required for complete matrix removal and quantitative Pb recovery (Fig. 2). This was done by loading such an amount of a soil (BCR CRM 141 Calcareous Loam Soil and BCR CRM 142 Light Sandy Soil) or bone (NIST SRM 1400 Bone Ash) digest in 1.0 M HNO_3 onto the column so that approximately 10 μg of Pb was present. The effluent was collected. Next, the column was rinsed with 20 mL 0.1 M HNO_3, in 1 mL aliquots and every 1 mL fraction was collected, followed by Pb elution with 20 mL 0.05 M $(NH_4)_2C_2O_4$ solution, where again every 1 mL fraction was collected separately. In the resulting 41 fractions (1 effluent, 20 rinse and 20 eluent fractions), Pb and other soil or bone matrix elements were determined semi-quantitatively. The elution profile for a BCR CRM 142 Light Sandy Soil sample is displayed in Fig. 2. Mg and Fe display no affinity for the column. K, Ca, Zn, Sr, Ba and Tl are retained by the column, but are completely removed during column rinse. The removal of matrix elements is complete after rinsing with 10 mL 0.1 M HNO_3, and the pure Pb fraction is completely recovered after elution with 10 mL 0.05 M $(NH_4)_2C_2O_4$ solution. Exactly the same elution profile and conclusion was found for a BCR CRM 141 Calcareous Loam Soil sample and a NIST SRM 1400 Bone Ash sample.

The isolation method developed was applied to the archaeological samples. Between 5 and 15 μg of Pb, depending on the Pb concentration in the sample, was loaded onto the column. The column recoveries for the samples were determined by comparing the Pb concentration in the digested sample and in the Pb fraction after the isolation process. This resulted in an

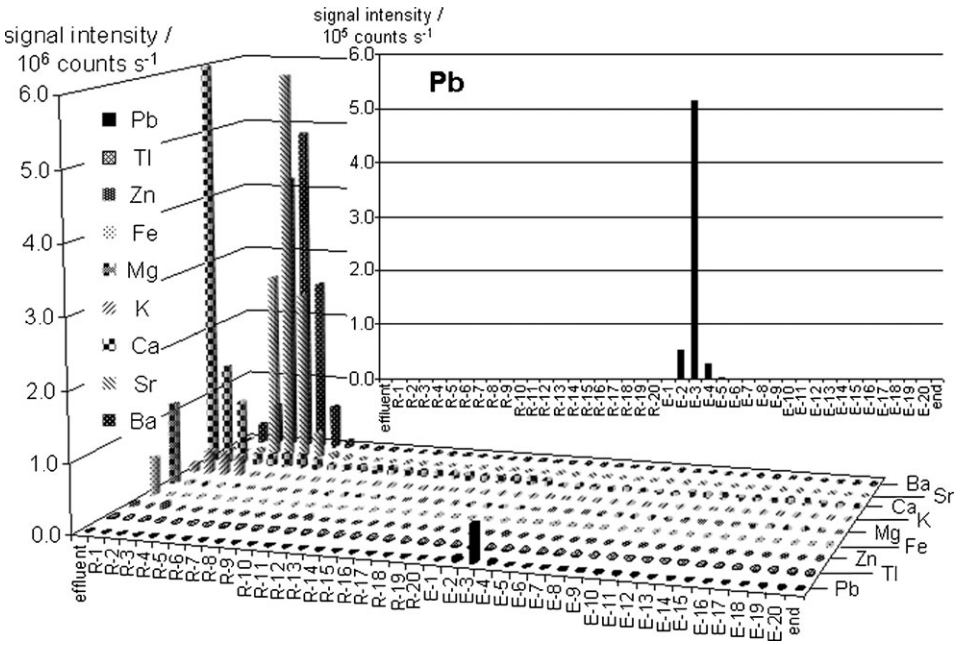

Fig. 2 Elution profile for a BCR CRM 142 Light Sandy Soil sample on Pb spec™. R − x = 1 mL 0.1 M HNO_3 rinse fraction x, E − x = 1 mL 0.05 M $(NH_4)_2C_2O_4$ elution fraction x.

experimental Pb recovery and 95% confidence interval of 99.8 ± 5.1% for bone tissue (n = 23), 100.3 ± 1.5% for soil (n = 22) and 100.0 ± 2.0% for amphorae (n = 9), leading to an average Pb recovery of 100.0 ± 2.1% (n = 54) on Pb spec™.

The elution profile on Pb spec™ (Fig. 2) shows that Sr is quantitatively retained after sample loading. This suggests that a methodology for the separation of Pb and Sr can be derived from this one. The rinse fraction can be considered as the Pb-free Sr fraction of the sample, which can be further purified using, *e.g.*, Sr spec™.

Isotopic fractionation induced on Pb spec™. As stated above, no measurable Pb isotopic fractionation is expected to occur. However, in this work (i) an amount of sample ranging from 0.1 to 10 mL depending on the Pb concentration present, was loaded onto the column. Furthermore, (ii) the column is higher than that used in the method of Manhès *et al.*[31] These 2 factors might induce isotopic fractionation. To verify that no Pb isotopic fractionation occurred during the isolation process, 10 μg Pb as a NIST SRM 981 Common Lead solution was conducted through the isolation process, followed by isotope ratio measurement using a Nu Plasma multi-collector ICP-MS (G. Quitté, ETH Zürich). The experimentally determined isotope ratio results for NIST SRM 981 Common Lead, before and after column chemistry, are given in Table 4a. The Pb isotope ratios obtained before and after the isolation process match within experimental error and are in agreement with the widely accepted values given by Galer and Abouchami.[37] However, the ratios with ^{204}Pb slightly shifted to a higher value, but stay within the experimental uncertainty. In view of the very good agreement for isotope ratios without ^{204}Pb, it can be concluded that there is no isotopic fractionation during the isolation process. The quantitative Pb recovery on Pb spec™ already pointed in this direction.

2.5. Optimization of single-collector ICP-DRC-MS

Detector dead time. The detector dead time was experimentally determined *via* 2 different methods,[38,39] and equalled 61 ± 2 ns.

Table 4 (a) Experimental Pb isotope ratio results obtained using MC-ICP-MS for NIST SRM 981 Common Lead before and after the isolation process; (b) Accuracy and external precision in % RSD (n = 40) for NIST SRM 981 Common Lead measured during a typical single-collector ICP-DRC-MS measurement session

	^{206}Pb/^{204}Pb		^{207}Pb/^{204}Pb		^{208}Pb/^{204}Pb		^{207}Pb/^{206}Pb		^{208}Pb/^{206}Pb		^{208}Pb/^{207}Pb	
	IR	2s	IR	2s	IR	2s	IR	2s	IR	2s	IR	2s
(a) Experimental Pb isotope ratios for NIST SRM 981 Common Lead via multi-collector ICP-MS[a]												
Before isolation process	16.9403	0.0084	15.4964	0.0057	36.7163	0.0100	0.91476	0.00010	2.16739	0.00043	2.3698	0.0002
After isolation process	16.9485	0.0099	15.5081	0.0130	36.7411	0.0252	0.91479	0.00019	2.16782	0.00061	2.3699	0.0003
Accepted value[37]	16.9405		15.4963		36.7219		0.91475		2.16771		2.3697	
(b) Accuracy and external precision (% RSD) for a typical single-collector ICP-DRC-MS measurement session												
Experimental ratio	16.9410	0.0537	15.4967	0.0469	36.7230	0.1228	0.91474	0.00172	2.16771	0.00256	2.3698	0.0036
External precision (% RSD)	0.16		0.15		0.17		0.09		0.06		0.08	

[a] The MC-ICP-MS measurements have been performed by G. Quitté at ETH Zürich.

Collision gas. Two inert gases, Ne and Ar, were examined as candidate collision gases with the intention to obtain an improved Pb isotope ratio precision compared to that attainable with standard quadrupole-based ICP-MS. The effect of three parameters on the Pb signal intensities and Pb isotope ratio precisions measured was investigated by registering the signals for ^{206}Pb, ^{207}Pb and ^{208}Pb while measuring a 25 μg L^{-1} NIST SRM 981 Common Lead solution. The influence of the collision gas flow rate on the Pb intensity was evaluated by varying the gas flow rate from 0.1 to 0.7 mL min^{-1}, in steps of 0.1 mL min^{-1} (Fig. 3a). At 0.1 mL min^{-1}, a signal decrease, compared to vented mode (no collision gas in the DRC), of 13% with Ar and 4% with Ne was observed. The higher the flow rate, the more Ar suppresses the Pb signals compared to Ne; at 0.7 mL min^{-1}, the suppression by Ar is 98% compared to 20% by Ne. This effect can be attributed to the higher mass of Ar ($\sim$40 u) compared to Ne ($\sim$20 u); scattering losses of Pb ions are less pronounced for the lighter collision gas Ne.

The precision attainable with a Ne- or Ar-pressurized cell was then compared to that typical for vented mode. The % RSD values, as a function of the Ne and Ar gas flow rate (0.1 to 0.7 mL min^{-1} per 0.1 mL min^{-1}), were determined for the $^{207}Pb/^{206}Pb$, $^{208}Pb/^{206}Pb$ (Fig. 3b) and $^{208}Pb/^{207}Pb$ ratios, and follow exactly the same pattern. For Ar, the Pb isotope ratio precision deteriorates with increasing gas flow rate, but for 0.1 mL min^{-1}, the precision is very similar to that obtained for Ne at the same flow rate. In the case of Ne, the precision remains constant in the range 0.1–0.6 mL min^{-1} at 0.12% RSD.

Finally, the mass discrimination effect due to the presence of a collision gas in the DRC[9] was also evaluated (Fig. 3c). At 0.1 mL min^{-1}, the raw $^{208}Pb/^{206}Pb$ ratio is—compared to vented mode—increased by 2% when Ne is used, and by 3% when Ar is used, and becomes higher at higher flow rates for both Ar and Ne. Since both isotopic standards and samples are measured under the same conditions, this observation can be accurately corrected for, as described in the next paragraph.

It can be concluded that (i) Ne is preferred over Ar owing to its (much) lower scattering losses, (ii) the same level of precision is obtained at a lower Ne gas flow rate, minimizing both scattering losses and gas consumption, and (iii) the mass discrimination effect induced by the use of a collision gas in the DRC is the lowest for Ne. As a consequence, Ne was selected as collision gas and was introduced into the DRC at a flow rate of 0.1 mL min^{-1}.

Measurement, data handling and mass discrimination correction. The instrumental settings and data-acquisition parameters for isotope ratio measurements are summarized in Table 1. The measurement sequence consisted of an on-peak blank measurement, followed by the samples, every time bracketed by a 25 μg L^{-1} NIST SRM 981 Common Lead solution in 0.14 M HNO_3. The samples, present in 0.05 M $(NH_4)_2C_2O_4$ after the isolation process, were diluted with 0.14 M HNO_3 to obtain a Pb concentration between 25 and 50 μg L^{-1}. The ratio of Pb intensities encountered for procedural blanks *versus* NIST SRM 981 Common Lead standards and samples was always lower than $4 \cdot 10^{-3}$, and it was observed that the same isotope ratio values were obtained

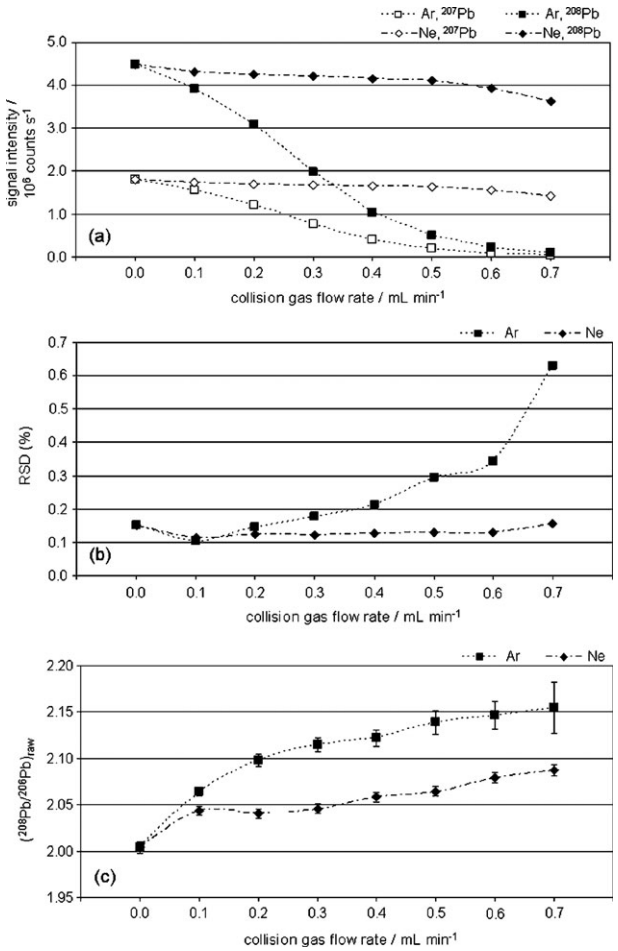

Fig. 3 (a) Pb signal intensities as a function of the collision gas flow rate; (b) % RSD for the $^{208}Pb/^{206}Pb$ ratio (n = 10) as a function of the collision gas flow rate; (c) Raw $^{208}Pb/^{206}Pb$ ratio as a function of the collision gas flow rate.

with and without blank correction. However, to be consistent, a blank correction was always performed.

The isotope ratio measurement consisted of 15 replicates of 46 s each, making a total sample time of $\sim$11 min. When the DRC is pressurized, the cell opens/closes at the start/end of every measurement, causing a 'delay time', before a homogeneous pressure within the cell is established again. As a consequence, considerable signal fluctuations can occur during the first 2–4 replicates, resulting in an isotope ratio precision that is up to 0.04% RSD better when only the last 10 replicates are considered. Thus, only replicates 6 to 15 were used for isotope ratio calculations, and the measurement time for the first 5 replicates should be regarded as a stabilization time.

The $^{206}Pb/^{204}Pb$, $^{207}Pb/^{204}Pb$, $^{208}Pb/^{204}Pb$, $^{207}Pb/^{206}Pb$, $^{208}Pb/^{206}Pb$ and $^{208}Pb/^{207}Pb$ ratios in the 10 replicates for both NIST SRM 981 Common Lead standards and samples were calculated. A Q-test on the 95% confidence interval was performed, but the occurrence of outliers was sporadic. The mean, standard deviation (2s) and relative standard deviation (% RSD) were calculated for every sample and standard. The raw sample ratios thus obtained were corrected for mass

discrimination *via* the external bracketing technique, thus the sample ratios ($R_{true,sample}$) were calculated as follows:

$$R_{true,sample} = R_{NIST,cert} \frac{R_{obs,sample}}{\frac{R_{NIST,before}+R_{NIST,after}}{2}}$$

where $R_{NIST,cert}$ is the commonly accepted value for NIST SRM 981 Common Lead given by Galer and Abouchami.[37] As the Pb concentration for the samples is higher than for the NIST SRM 981 Common Lead standards, it can be assumed that the external precision calculated from the NIST SRM 981 Common Lead standards is a "worst case" limit for the precision of the samples (counting statistics), and thus the internal precision for the samples should be as good as, or better than, the external precision. The internal precision (% RSD) was shown to be typically 0.15–0.17% for ratios with ^{204}Pb, and 0.06–0.09% for the other ratios. The external precision for the entire session was calculated *via* the NIST SRM 981 Common Lead standards (Table 4b), and was found to be as good as the internal precision. Literature Pb isotope ratio precision values obtained *via* sector field ICP-MS cover the range of 0.04–0.27% RSD.[40–42] The use of ICP-DRC-MS for Pb isotope ratio measurements in peat cores has been reported on by Jackson *et al.*[43] The use of an Ar–H_2 mixture at a gas flow rate of 0.5 mL min^{-1} resulted in a Pb isotope ratio precision below 0.5% RSD for the ratios without ^{204}Pb for the samples (no information on the ^{204}Pb isotope was reported), and below 0.1% RSD for the ^{206}Pb/^{207}Pb ratio for the NIST SRM 981 Common Lead standards. The quadrupole-based method developed here offers a Pb isotope ratio precision that is similar to or better than the best results reported for sector field ICP-MS and ICP-DRC-MS. Furthermore, the ratios with ^{204}Pb can also be successfully determined.

3. Results and discussion

The accuracy of the single-collector ICP-DRC-MS measurement protocol developed has been validated by comparing the data obtained to the corresponding values obtained *via* multi-collector ICP-MS. The accuracy and reproducibility of the complete method (Pb isolation + single-collector ICP-DRC-MS measurement) has been validated by (i) duplicate analyses of bone and soil samples using single-collector ICP-DRC-MS and (ii) application of the method to a completely different, but also complex, reference material: BCR CRM 482 Lichen. The method was finally applied to the determination of the Pb isotopic composition for the bone and soil certified reference materials used in this work.

3.1 Duplo analyses

The results for duplicate analyses of bone and soil samples are given in Table 5. Every time, the single-collector ICP-DRC-MS duplicate analyses match within error. An average bias of 0.27% for ^{206}Pb/^{204}Pb, 0.22% for ^{207}Pb/^{204}Pb, 0.07% for ^{208}Pb/^{204}Pb, 0.09% for ^{207}Pb/^{206}Pb, 0.17% for ^{208}Pb/^{206}Pb and 0.13% for ^{208}Pb/^{207}Pb is observed. The bias between duplicate analyses is within the external precision of the method. Nevertheless, for 1 sample, a bias between duplicate results of 0.42% on the ^{208}Pb/^{206}Pb ratio was observed. This bias can most likely be attributed to the heterogeneity of the samples, since, as is shown below, the method can be considered as accurate and reproducible.

3.2 Comparison of single-collector and multi-collector ICP-MS results

A comparison between results obtained *via* single-collector ICP-DRC-MS and multi-collector ICP-MS for some bone, soil, amphora and lead object samples, chosen on the basis of their different Pb isotopic composition, is given in Table 5. It can be seen that, within error, every single isotope ratio obtained *via* SC-ICP-DRC-MS matches the corresponding MC-ICP-MS result, including those with ^{204}Pb. One of both duplicates, mentioned in the previous paragraph, was also analyzed *via* MC-ICP-MS. For every sample where the SC-ICP-DRC-MS and MC-ICP-MS results are compared, a maximal discrepancy between SC-ICP-DRC-MS and MC-ICP-MS results of 0.18% for ^{206}Pb/^{204}Pb and ^{207}Pb/^{204}Pb, 0.24% for ^{208}Pb/^{204}Pb, 0.08% for ^{207}Pb/^{206}Pb, 0.09% for ^{208}Pb/^{206}Pb and 0.06% for ^{208}Pb/^{207}Pb is observed. Moreover, the dispersion of Pb isotope ratios among the displayed samples is larger than the attainable precision *via* SC-ICP-DRC-MS (Table 5). As a conclusion, it can be stated that (i) the single-collector ICP-MS measurement protocol leads to accurate results and (ii) the method developed is fit-for-purpose.

3.3 Pb isotope ratio determination in reference materials

Pb isotope ratio results for the reference materials analyzed in this work are summarized in Table 6. As a part of another research project, currently being carried out in our lab, Pb isotope ratio analysis of a lichen reference material (BCR CRM 482 Lichen) was performed. Cloquet *et al.*[44] published Pb isotope ratios for this material, obtained *via* a Micromass Isoprobe multi-collector ICP-MS. The lichen reference material was digested as described in the paper cited above, followed by the extraction chromatographic separation and the single-collector ICP-DRC-MS analytical protocol developed here. As can be seen from Table 6, there is an excellent agreement between the new single-collector ICP-DRC-MS data on one hand, and the multi-collector ICP-MS data on the other hand. This suggests that the method can be successfully applied for a wide range of Pb isotopic analysis applications in heavy matrices.

Hinners *et al.*[22] already published Pb isotope ratios for NIST SRM 1400 Bone Ash obtained *via* TI-MS, based on the NIST SRM 981 Common Lead DS-TI-MS values reported by Woodhead *et al.*[45] In Table 6, the values of Hinners *et al.*[22] have been recalculated using the more recent NIST SRM 981 Common Lead TS-TI-MS values as given by Galer and Abouchami,[37] to be consistent with the normalization used throughout this work. The single-collector ICP-DRC-MS results for NIST SRM 1400 Bone Ash are in very good agreement with the TI-MS values, confirming the method's reliability for Pb isotope ratio analysis.

Table 5 Duplicate analyses for bone and soil samples and comparison of single-collector ICP-DRC-MS and multi-collector ICP-MS Pb isotope ratio results for selected archaeological samples

		$^{206}Pb/^{204}Pb$		$^{207}Pb/^{204}Pb$		$^{208}Pb/^{204}Pb$		$^{207}Pb/^{206}Pb$		$^{208}Pb/^{206}Pb$		$^{208}Pb/^{207}Pb$	
		IR	2*s*	IR	2*s*	IR	2*s*	IR	2*s*	IR	2*s*	IR	2*s*
Bone samples[a]													
6-265-328	SC[b]	18.644	0.059	15.688	0.047	38.537	0.129	0.8408	0.0016	2.0671	0.0024	2.4586	0.0037
	SC-duplo	18.590	0.046	15.615	0.035	38.478	0.109	0.8399	0.0013	2.0684	0.0024	2.4626	0.0037
	MC	18.632	0.007	15.644	0.006	38.577	0.015	0.8397	0.0001	2.0705	0.0002	2.4659	0.0002
13-2-236	SC[b]	18.416	0.059	15.635	0.047	38.438	0.114	0.8489	0.0016	2.0853	0.0025	2.4564	0.0037
	SC-duplo	18.436	0.059	15.647	0.047	38.430	0.128	0.8487	0.0016	2.0845	0.0025	2.4561	0.0037
	MC	18.435	0.007	15.638	0.006	38.436	0.015	0.8483	0.0001	2.0849	0.0002	2.4578	0.0002
14-152-202	SC	18.598	0.058	15.647	0.042	38.597	0.097	0.8412	0.0013	2.0741	0.0025	2.4658	0.0036
	MC	18.599	0.007	15.654	0.006	38.609	0.015	0.8417	0.0001	2.0757	0.0002	2.4662	0.0002
51-60-176	SC	18.506	0.059	15.625	0.047	38.473	0.129	0.8445	0.0013	2.0799	0.0025	2.4634	0.0036
	MC	18.529	0.007	15.652	0.006	38.566	0.015	0.8448	0.0001	2.0815	0.0002	2.4640	0.0002
Soil samples[a]													
1-140-165	SC	18.899	0.055	15.693	0.045	38.803	0.109	0.8300	0.0009	2.0527	0.0024	2.4721	0.0038
	SC-duplo[b]	18.819	0.060	15.652	0.047	38.794	0.130	0.8317	0.0010	2.0607	0.0020	2.4777	0.0036
	MC	18.845	0.007	15.662	0.006	38.847	0.015	0.8311	0.0001	2.0614	0.0002	2.4804	0.0002
6-99-128	SC	18.384	0.059	15.626	0.047	38.383	0.128	0.8497	0.0014	2.0878	0.0025	2.4567	0.0028
	MC	18.385	0.007	15.624	0.006	38.380	0.015	0.8499	0.0001	2.0871	0.0002	2.4557	0.0002
6-265-328	SC	18.815	0.060	15.626	0.047	38.695	0.129	0.8324	0.0014	2.0566	0.0024	2.4722	0.0038
	SC-duplo[b]	18.764	0.050	15.617	0.044	38.729	0.116	0.8323	0.0012	2.0605	0.0024	2.4756	0.0038
	MC	18.834	0.007	15.654	0.006	38.782	0.015	0.8315	0.0001	2.0592	0.0002	2.4775	0.0002
71-29-54	SC	18.730	0.054	15.667	0.048	38.746	0.101	0.8365	0.0013	2.0683	0.0024	2.4731	0.0034
	MC	18.718	0.007	15.661	0.006	38.748	0.015	0.8367	0.0001	2.0701	0.0002	2.4742	0.0002
Amphorae[a]													
C-3656	SC	18.599	0.059	15.672	0.047	38.600	0.127	0.8429	0.0016	2.0780	0.0025	2.4653	0.0038
	MC	18.572	0.007	15.657	0.006	38.597	0.015	0.8430	0.0001	2.0782	0.0002	2.4653	0.0002
C-3668	SC	18.811	0.060	15.689	0.047	38.808	0.130	0.8338	0.0010	2.0644	0.0024	2.4762	0.0027
	MC	18.796	0.007	15.670	0.006	38.799	0.015	0.8337	0.0001	2.0642	0.0002	2.4761	0.0002
Lead objects[a]													
3-2-32	SC	18.414	0.059	15.640	0.047	38.416	0.081	0.8494	0.0011	2.0880	0.0025	2.4583	0.0037
	MC	18.411	0.007	15.639	0.006	38.420	0.015	0.8493	0.0001	2.0871	0.0002	2.4572	0.0002
6-62-20	SC	18.398	0.057	15.627	0.047	38.414	0.124	0.8499	0.0016	2.0878	0.0024	2.4568	0.0037
	MC	18.395	0.007	15.624	0.006	38.394	0.015	0.8498	0.0001	2.0872	0.0002	2.4565	0.0002

[a] The MC-ICP-MS measurements have been performed by G. Quitté at ETH Zürich. [b] The MC-ICP-MS result reported was obtained for this sample.

For the soil reference materials BCR CRM 141 Calcareous Loam Soil and BCR CRM 142 Light Sandy Soil, no Pb isotopic composition has been published so far.

3.4 Regeneration of extraction chromatographic columns

An experiment was set up to (i) assess the performance of the extraction chromatographic column after being regenerated, *i.e.*, when it is used a second time, and (ii) to test whether there is a change in recovery and/or isotope ratio, when the column is applied for a second time for a matrix different from that when the column was used for the first time. An experiment involving 5 columns was carried out. In a first batch, an amount of dissolved NIST SRM 1400 Bone Ash (2×), BCR CRM 141 Calcareous Loam Soil (1×) and BCR CRM 142 Light Sandy Soil (2×) was loaded onto a column. After the isolation procedure, the column was washed with 100 mL Milli-Q water. This regeneration procedure was suggested by Horwitz *et al.*,[32] but since bone and soil are quite complex matrices, it could not be simply taken for granted that this regeneration step would be sufficient. In a second batch, an amount of NIST SRM 1400 Bone Ash (2×, same columns as 1st batch), BCR CRM 141 Calcareous Loam Soil (2×, once on same column, once on BCR CRM 142 Light Sandy Soil column from 1st batch) and BCR CRM 142 Light Sandy Soil (1×, same column as 1st batch) was loaded onto the column followed by the isolation procedure. Horwitz *et al.*[32] stated that, in case of a second column use, the Pb elution profile shifts to a slightly higher volume before complete elution is accomplished (shift $\leq$1 mL), but here, 10 mL 0.05 M $(NH_4)_2C_2O_4$ solution was observed to remain sufficient for quantitative Pb recovery. The isotope ratio results for the column regeneration experiment are given in Table 6. For every digestion, the mean of 2 duplicate analyses is reported. No systematic trend is observed between the isotope ratio results for (i) the first and second use of the column and (ii) the result for BCR CRM 141 Calcareous Loam after separation on a column where BCR CRM 142 Light Sandy Soil was loaded in the previous batch. Thus, there is no objection against regenerating a column and using it for a second Pb isolation, even when very complex matrices are subject to study, as no effect on both recovery and isotope ratios could be established. A 2nd and higher regeneration has not been tested, in these cases one has to take care about a further shift of the Pb elution profile to a higher volume before elution is complete. From the observation that the elution of Pb is complete after 5 mL after the 1st regeneration, a 2nd regeneration of the column should still display the same performance when elution is done with 10 mL $(NH_4)_2C_2O_4$ solution.

Table 6 Pb isotope ratios for reference materials BCR CRM 482 Lichen, NIST SRM 1400 Bone Ash, BCR CRM 141 Calcareous Loam Soil and BCR CRM 142 Light Sandy Soil

		$^{206}Pb/^{204}Pb$		$^{207}Pb/^{204}Pb$		$^{208}Pb/^{204}Pb$		$^{207}Pb/^{206}Pb$		$^{208}Pb/^{206}Pb$		$^{208}Pb/^{207}Pb$	
		IR	2*s*	IR	2*s*	IR	2*s*	IR	2*s*	IR	2*s*	IR	2*s*
BCR CRM 482 Lichen													
SC-ICP-DRC-MS (n=3)		*17.607*	*0.114*	*15.568*	*0.061*	*37.495*	*0.235*	*0.8842*	*0.0024*	*2.1296*	*0.0012*	*2.4085*	*0.0047*
MC-ICP-MS ($n = 4$)[44]		17.611	0.007	15.570	0.007	37.490	0.020	0.8841	0.0001	2.1288	0.0003	2.4078	0.0004
NIST SRM 1400 Bone ash													
Column 1–pass 1	BA–1[a]	18.368	0.071	15.680	0.075	38.626	0.207	0.8536	0.0008	2.1031	0.0026	2.4635	0.0014
Column 1–pass 2	BA–2[a]	18.333	0.044	15.655	0.030	38.561	0.013	0.8546	0.0018	2.1047	0.0019	2.4631	0.0039
Column 2–pass 1	BA–3[a]	18.357	0.053	15.684	0.030	38.604	0.150	0.8543	0.0008	2.1026	0.0008	2.4605	0.0019
Column 2–pass 2	BA–4[a]	18.363	0.069	15.676	0.039	38.631	0.062	0.8537	0.0011	2.1038	0.0046	2.4644	0.0022
SC-ICP-DRC-MS (n = 4)		*18.355*	*0.031*	*15.674*	*0.025*	*38.606*	*0.064*	*0.8541*	*0.0010*	*2.1036*	*0.0019*	*2.4629*	*0.0033*
TI-MS ($n = 7$)[22]		18.371	0.014	15.675	0.012	38.625	0.040	0.8532	0.0002	2.1025	0.0007	2.4642	0.0003
BCR CRM 141 Calcareous loam soil													
Column 3–pass 1	CLS–1[a]	18.607	0.097	15.670	0.078	38.637	0.186	0.8421	0.0002	2.0762	0.0002	2.4663	0.0011
Column 3–pass 2	CLS–2[a]	18.604	0.076	15.688	0.082	38.715	0.188	0.8433	0.0010	2.0803	0.0004	2.4673	0.0025
Column 4–pass 2	CLS–3[a]	18.589	0.044	15.643	0.041	38.578	0.044	0.8419	0.0013	2.0766	0.0050	2.4667	0.0077
SC-ICP-DRC-MS (n = 3)		*18.600*	*0.019*	*15.667*	*0.046*	*38.643*	*0.138*	*0.8424*	*0.0015*	*2.0777*	*0.0045*	*2.4667*	*0.0010*
BCR CRM 142 Light sandy soil													
Column 4–pass 1	LSS–1[a]	18.546	0.020	15.638	0.014	38.585	0.050	0.8432	0.0002	2.0810	0.0006	2.4674	0.0011
Column 5–pass 1	LSS–2[a]	18.529	0.073	15.666	0.049	38.625	0.152	0.8454	0.0009	2.0842	0.0010	2.4653	0.0044
Column 5–pass 2	LSS–3[a]	18.530	0.029	15.653	0.034	38.537	0.078	0.8446	0.0002	2.0791	0.0015	2.4610	0.0040
SC-ICP-DRC-MS (n = 3)		*18.535*	*0.019*	*15.652*	*0.028*	*38.582*	*0.089*	*0.8444*	*0.0022*	*2.0814*	*0.0051*	*2.4646*	*0.0065*

[a] Mean value of 2 duplicate sample measurements.

4. Conclusions

A new methodology has been developed for Pb isotope ratio analysis of archaeological samples, but it has been proved that the method is applicable for a wide range of applications (beyond archaeology), in which Pb isotope ratio analysis is required and for which an excellent precision as offered by MC-ICP-MS is not mandatory. An extraction chromatographic procedure was optimized, in which less harmful chemicals are used than in previously described isolation procedures. Furthermore, it was shown that regeneration of the columns used is possible, without a loss of separation efficiency or influence on isotope ratios. The single-collector ICP-MS measurement protocol, using Ne as a collision gas in a DRC, was shown to be accurate and reproducible, with Pb isotope ratio results similar to multi-collector ICP-MS and TI-MS results, including the ratios with ^{204}Pb. This method is also more precise than 'traditional' quadrupole-based ICP-MS. Finally, Pb isotope ratios were reported for 4 certified reference materials. Two of them were soils, of which the Pb isotopic composition had not been reported on so far.

The full set of data for the bone tissue, soil, amphora samples and Pb objects investigated, will be published in a later paper, currently in preparation. The method reported on here will also be applied for Pb isotopic studies on metallic objects, such as coins, Cu–Ag alloy objects and silver rings, as a part of another archaeological research project currently being carried out in our lab.

Acknowledgements

The authors thank Dr Ghylaine Quitté (ETH Zürich, presently: CNRS Lyon) for the MC-ICP-MS measurements. Dr Elisabeth Smits (University of Amsterdam) is acknowledged for providing the archaeological samples. D.D.M. thanks the Special Research Fund (Bijzonder Onderzoeksfonds, grant B/05608/01) from Ghent University for financial support. F.V. acknowledges the Fund for Scientific Research–Flanders (FWO-Vlaanderen) for financial support (FWO project G.0669.06).

References

1 T. Walczyk, *Anal. Bioanal. Chem.*, 2004, **378**, 229–231.
2 K. G. Heumann, S. M. Gallus, G. Rädlinger and J. Vogl, *J. Anal. At. Spectrom.*, 1998, **13**, 1001–1008.
3 F. Vanhaecke, L. Moens, R. Dams and P. Taylor, *Anal. Chem.*, 1996, **68**, 567–569.
4 I. Feldmann, N. Jakubowski and D. Stuewer, *Fresenius' J. Anal. Chem.*, 1999, **365**, 415–421.
5 I. Feldmann, N. Jakubowski, C. Thomas and D. Stuewer, *Fresenius' J. Anal. Chem.*, 1999, **365**, 422–428.
6 D. W. Koppenaal, G. C. Eiden and C. J. Barinaga, *J. Anal. At. Spectrom.*, 2004, **19**, 561–570.
7 S. D. Tanner and V. I. Baranov, *At. Spectrosc.*, 1999, **20**, 45–52.
8 D. R. Bandura and S. D. Tanner, *At. Spectrosc.*, 1999, **20**, 69–72.
9 F. Vanhaecke, L. Balcaen, I. Deconinck, I. De Schrijver, C. M. Almeida and L. Moens, *J. Anal. At. Spectrom.*, 2003, **18**, 1060–1065.
10 A. D. Anbar, J. E. Roe, J. Barling and K. H. Nealson, *Science*, 2000, **288**, 126–128.
11 C. Maréchal and F. Albarède, *Geochim. Cosmochim. Acta*, 2002, **66**, 1499–1509.
12 C. Cloquet, O. Rouxel, J. Carignan and G. Libourel, *Geostand. Geoanal. Res.*, 2005, **29**, 95–106.
13 K. J. R. Rosman and P. D. P. Taylor, *Pure Appl. Chem.*, 1998, **70**, 217–235.
14 K. J. Reinhard and A. M. Ghazi, *Am. J. Phys. Anthropol.*, 1992, **89**, 183–195.

15 G. Aberg, G. Fosse and H. Stray, *Sci. Total Environ.*, 1998, **224**, 109–119.
16 N. W. Bower, S. R. Getty, C. P. Smith, Z. R. Simpson and J. M. Hoffman, *Int. J. Osteoarchaeol.*, 2005, **15**, 360–370.
17 N. W. Bower, S. A. McCants, J. M. Custodio, M. E. Ketterer, S. R. Getty and J. M. Hoffman, *Sci. Total Environ.*, 2007, **372**, 463–473.
18 D. R. Bandura, V. I. Baranov and S. D. Tanner, *J. Anal. At. Spectrom.*, 2000, **15**, 921–928.
19 S. D. Tanner, V. I. Baranov and D. R. Bandura, *Spectrochim. Acta, Part B*, 2002, **57**, 1361–1452.
20 L. J. Moens, F. F. Vanhaecke, D. R. Bandura, V. I. Baranov and S. D. Tanner, *J. Anal. At. Spectrom.*, 2001, **16**, 991–994.
21 J. Latino, K. Neubauer and R. E. Wolf, *At. Spectrosc.*, 2001, **22**, 306–311.
22 T. A. Hinners, R. Hughes, P. M. Outridge, W. J. Davis, K. Simon and D. R. Woolard, *J. Anal. At. Spectrom.*, 1998, **13**, 963–970.
23 M. Bettinelli, C. Baffi, G. M. Beone and S. Spezia, *At. Spectrosc.*, 2000, **21**, 50–59.
24 R. Falciani, E. Novaro, M. Marchesini and M. Gucciardi, *J. Anal. At. Spectrom.*, 2000, **15**, 561–565.
25 E. Engström, A. Stenberg, D.C. Baxter, D. Malinovsky, I. Mäkinen, S. Pönni and I. Rodushkin, *J. Anal. At. Spectrom.*, 2004, **19**, 858–866.
26 J. Riondato, F. Vanhaecke, L. Moens and R. Dams, *Fresenius' J. Anal. Chem.*, 2001, **370**, 544–552.
27 L. M. Mallory-Greenough, J. D. Greenough and J. V. Owen, *J. Archaeol. Sci.*, 1998, **25**, 85–97.
28 D. J. Kennett, A. J. Anderson, M. J. Cruz, G. R. Clark and G. R. Summerhayes, *Archaeometry*, 2004, **46**, 35–46.
29 N. C. Little, L. J. Kosakowsky, R. J. Speakman, M. D. Glascock and J. C. Lohse, *J. Radioanal. Nucl. Chem.*, 2004, **262**, 103–110.
30 E. Marengo, M. Aceto, E. Robotti, M. C. Liparota, M. Bobba and G. Pantó, *Anal. Chim. Acta*, 2005, **537**, 359–375.
31 G. Manhès, C. J. Allègre, B. Dupré and B. Hamelin, *Earth Planet. Sci. Lett.*, 1980, **47**, 370–382.
32 E. P. Horwitz, M. L. Dietz, S. Rhoads, C. Felinto, N. H. Gale and J. Houghton, *Anal. Chim. Acta*, 1994, **292**, 263–273.
33 C. Pin and C. Bassin, *Anal. Chim. Acta*, 1992, **269**, 249–255.
34 J. Baker, D. Peate, T. Waight and C. Meyzen, *Chem. Geol.*, 2004, **211**, 275–303.
35 G. D. Kamenov, P. A. Mueller and M. R. Perfit, *J. Anal. At. Spectrom.*, 2004, **19**, 1262–1267.
36 D. J. Weiss, B. Kober, A. Dolgopolova, K. Gallagher, B. Spiro, G. Le Roux, T. F. D. Mason, M. Kylander and B. J. Coles, *Int. J. Mass Spectrom.*, 2004, **232**, 205–215.
37 S. J. G. Galer and W. Abouchami, *Mineral. Mag.*, 1998, **62A**, 491–492.
38 G. P. Russ III, in *Applications of inductively coupled plasma mass spectrometry*, ed. A.R. Date and A.L. Gray, Blackie, Glasgow, 1989, ch. 4, pp. 90–114.
39 S. M. Nelms, C. R. Quétel, T. Prohaska, J. Vogl and P. D. P. Taylor, *J. Anal. At. Spectrom.*, 2001, **16**, 333–338.
40 D. Woolard, R. Franks and D. R. Smith, *J. Anal. At. Spectrom.*, 1998, **13**, 1015–1019.
41 G. De Wannemacker, F. Vanhaecke, L. Moens, A. Van Mele and H. Thoen, *J. Anal. At. Spectrom.*, 2000, **15**, 323–327.
42 M. Krachler, G. Le Roux, B. Kober and W. Shotyk, *J. Anal. At. Spectrom.*, 2004, **19**, 354–361.
43 B. P. Jackson, P. V. Winger and P. J. Lasier, *Environ. Pollut.*, 2004, **130**, 445–451.
44 C. Cloquet, J. Carignan and G. Libourel, *Atmos. Environ.*, 2006, **40**, 574–587.
45 J. D. Woodhead, F. Volker and M. T. McCulloch, *Analyst*, 1995, **120**, 35–39.